Loss of iron to gold capsules in rock-melting experiments

KENT RATAJESKI[1],* AND THOMAS W. SISSON[2]

[1]Department of Geological Sciences, University of North Carolina, Chapel Hill, North Carolina 27599, U.S.A.
[2]Volcano Hazards Program, United States Geological Survey, Menlo Park, California 94025, U.S.A.

ABSTRACT

Gold is used widely for capsules in high-temperature rock-melting studies because it is generally thought to absorb negligible Fe from silicate samples. However, we observed significant losses of Fe from fluid-absent melting experiments on hornblende gabbros at 800–975 °C and 8 kbar, using standard piston-cylinder techniques. The extent of Fe loss from the sample is dependent on the relative masses of the sample and the capsule. Low sample to capsule mass ratios (~0.04) lead to the highest Fe losses (32–49% relative). Concentrations of Fe in silicate melt and used gold capsules define an apparent equilibrium constant (K') that follows a linear ln K' vs. $1/T$ relation (at an estimated log f_{O_2} of QFM-1). The apparent equilibrium constant is used to make limiting upper estimates on the amount of Fe that could be lost during rock-melting experiments for a range of f_{O_2} and sample to capsule mass ratios. At high f_{O_2} (NNO + 2), loss of Fe to gold is negligible (<2% relative) for a wide range of sample to capsule mass ratios. At an f_{O_2} of NNO, Fe loss can be kept to <10% relative by using a sample to capsule mass ratio of 0.2 or greater. At low f_{O_2} (QFM-1), presaturating the Au with Fe would be necessary to ensure that Fe losses remained <10% relative. Fe loss can compromise experimental results for small samples run at low f_{O_2} conditions, be they buffered, imposed by the pressure media, or produced by intrinsically reduced (graphitic) starting materials.

INTRODUCTION

Gold has found wide application as a material for sample containers in rock-melting and other high-temperature phase equilibrium experiments because it is nearly inert, is easily fabricated, has low H_2 diffusivity, and has particularly low Fe solubility compared to other noble metals and alloys. Although the absorption of Fe into Pt, Ag-Pd, and Au-Pd containers has been studied extensively (Merrill and Wyllie 1973; Nehru and Wyllie 1975; Stern 1973; Stern and Wyllie 1975; Grove 1981; Kawamoto and Hirose 1994; Gaetani and Grove 1998), much less has been published about the loss of Fe into Au capsules. A review of the literature indicates that nearly all experimental studies involving Au capsules do not even mention Fe loss (e.g., Vielzeuf and Holloway 1988; Patiño Douce and Beard 1995; Rapp and Watson 1995; Skjerlie and Johnston 1996), indicating either that Fe loss was not evaluated or was found not to be a problem. A few studies (Sisson and Grove 1993a, 1993b) apply mass-balance calculations and microprobe analyses of the used capsules to demonstrate minimal Fe losses (<10% relative) in their experiments. To our knowledge, the only example of significant Fe absorbtion by Au capsules reported in the literature is that of Le Breton and Thompson (1988) in which Fe loss was suggested as a possible cause of relatively high values for Fe-Mg exchange K_d calculated for coexisting garnet and biotite.

During the course of an experimental study of the melting behavior of hornblende gabbros, employing standard piston-cylinder techniques, we discovered that Fe was being absorbed by Au capsules to a degree that was obvious and that compromised the experimental results. We employed small Au capsules (1.4 mm inner diameter and 0.2 mm thick walls) so that we could run three starting compositions at the same time in each experiment. Low sample to capsule mass ratios (~0.04) were a consequence of this approach. Subsequent to discovering the Fe loss problem, we repeated the experiments using larger diameter capsules (2.5 and 4 mm inner diameter with 0.3 mm thick walls) that increased the sample to capsule mass ratio (~0.12–0.2) and reduced Fe loss considerably. The petrologic significance of our experimental study will be reported elsewhere. Here we analyze in detail the Fe loss relations in experiments on one of our starting compositions and use these to develop a framework for understanding Fe loss to Au in rock-melting experiments. Our purpose is to present simple thermodynamically based and experimentally calibrated relations that will enable researchers to design and conduct experiments in Au capsules with minimal Fe losses.

EXPERIMENTAL AND ANALYTICAL METHODS

Piston-cylinder experiments were carried out at the U.S. Geological Survey (USGS) at Menlo Park, California, on a natural hornblende quartz gabbro (YOS-55a; Table 1) collected from western Yosemite Valley in the central Sierra Nevada batholith, California. Initial experiments were performed in "small" (1.4 mm inner diameter with 0.2 mm thick walls) Au capsules, but after discovering that these experiments had lost significant amounts of Fe (see below), additional experiments

---

*E-mail: plutonic@email.unc.edu

TABLE 1. Modal and major-elemental compositon of starting material YOS-55a

Mode	vol%	Composition	wt%
Plagioclase	49	SiO_2	54.0(2)
Hornblende	32	TiO_2	1.03(2)
Quartz	8	Al_2O_3	17.9(0)
Biotite	7	FeO(tot)	8.11(9)
Chlorite	3	MnO	0.15(0)
Potassium feldspar	<1	MgO	5.43(6)
Ilmenite	<1	CaO	9.33(12)
Titanite	<1	Na_2O	2.74(4)
Total	99	K_2O	1.19(1)
		P_2O_5	0.21(2)
		Total	100.09

Notes: Standard deviations in the last decimal place (n = 3) are given in parentheses. Major-element analysis by DCP.

were run with "medium" and "large" capsules (2.5 and 4.0 mm inner diameter with 0.3 mm walls, respectively). Physical conditions (P, T, t) for all experiments are shown in Table 2. Loaded capsules were crimped closed and dried for at least one hour at 110 °C to expel adsorbed water before being welded shut. Charges were packed in powdered boron nitride inside a 2.54 cm diameter NaCl-graphite furnace assembly. Temperatures in the assemblies were measured and controlled with Pt-$Pt_{90}Rh_{10}$ thermocouples, and pressures were calibrated from prior alkali-halide melting-point determinations (Bohlen 1984) spanning the temperature range of the experiments. Samples were pressurized at room T to about 2/3–3/4 of the target pressure, then heated to 970 °C and pressure adjusted to final P (8 kbar). After stabilizing for 1 day, the temperature was adjusted to the final T. Run durations (at final T) ranged from 5 days to two weeks. For most experiments, equilibrium was approached from the high-T side (crystallization), but two melting experiments were also performed at 825 and 975 °C. One experiment (Run 33) was quenched after remaining at 970 °C for only one day to evaluate the amount of Fe lost during the early part of the experimental procedure.

Melting took place under fluid-absent conditions, and no effort was made to buffer the f_{O_2} of the samples. Patiño Douce and Beard (1994, 1995) determined f_{O_2} values of QFM to QFM-2 during fluid-absent melting of quartz amphibolite and biotite gneiss that were encapsulated in Au and run in NaCl-graphite piston cylinder furnace assemblies similar to those we em-

ployed. Patiño Douce and Beard (1994) documented the gradual desiccation and oxidation of samples melted for long durations in Au capsules and inferred that these changes resulted from diffusion of both H_2 and H_2O out of the capsule walls. Truckenbrodt et al. (1997) found that imbedding sample capsules in boron nitride reduced volatile transport through capsule walls to below measurement resolution, and we used boron nitride packing to minimize sample desiccation. Although Patiño Douce and Beard (1994, 1995) did not utilize boron nitride, their f_{O_2} estimates are the most comprehensive ones yet determined for samples, capsules, and furnace assemblies closely similar to those we employed, and we assume that our samples were melted at ~QFM-1.

Phases synthesized in the experiments were analyzed by wavelength-dispersive techniques with the five-spectrometer JEOL JXA-8900 electron microprobe at the USGS and the four-spectrometer CAMECA Camebax electron microprobe at Duke University. Instrumental conditions for the analysis of quenched melt pools were 15 kV accelerating potential, 2 nA beam current, 8 μm spot size, 5 or 10 s counting time for Na (analyzed first), and 20 s counting times for all other elements. A series of time-dependent measurements and analyses of standards (hydrous and anhydrous rhyolitic and basaltic glasses) indicated that Na migration was not analytically significant at these conditions. Reported glass compositions (Table 3) are means of 12–23 replicate analyses taken throughout each sample. Standard errors $\left(^{s}\!/_{\sqrt{n}} \right)$ in weight percent for 17 replicate analyses of USGS rhyolite glass standard RLS-132 are SiO_2, 0.11; TiO_2, 0.04; Al_2O_3, 0.08; FeO, 0.05; MnO, 0.03; MgO, 0.01; CaO, 0.01; Na_2O, 0.07; K_2O, 0.04; P_2O_5, 0.01. Instrumental conditions for the analysis of crystalline phases were 15 kV accelerating potential, 25 nA (plagioclase) or 30 nA (oxide, amphibole, and pyroxenes) beam current, ~1 μm spot size, 10 s counting time for Na (analyzed first), and 20 s counting times for all other elements. Standards were analyzed as unknowns prior to and interspersed with analyses of run products to monitor instrument drift.

Used and unused Au capsules were analyzed for Fe and Au with the JEOL JXA-8900 electron microprobe at the USGS. Analytical conditions were 30 kV accelerating potential, 200 nA beam current, and ~1 μm spot size. Iron was analyzed with

TABLE 2. Experimental conditions

Run no.	Capsule mass (g)	Sample mass (g)	Sample: capsule mass ratio	Initial T (°C)	Duration at initial T (days)	Final T (°C)	Duration at final T (days)
			1.4 mm capsule size				
Run 6	0.24017	0.01052	0.044	970	1	800	5
Run 10	0.25046	0.01045	0.042	970	1	950	4
Run 12	0.25744	0.01012	0.039	–	–	975	4
Run 16	0.20867	0.01067	0.051	970	1	800	14
			2.5 mm capsule size				
Run 25	0.43699	0.08758	0.200	970	1	800	14
Run 27	0.41360	0.07587	0.183	970	1	825	14
			4.0 mm capsule size				
Run 29	1.18973	0.12951	0.109	970	1	850	14
Run 33	1.31900	0.15360	0.116	–	–	970	1
Run 35	0.91432	0.13002	0.142	–	–	825	9

Note: All experiments at 8 kbar.

a high-resolution LiFH crystal spectrometer and standardized on pure Fe metal. Iron peaks were counted for 60 s and backgrounds for 30 s. Gold was standardized against a pure Au standard, and Au peaks were analyzed with a LiF crystal for 30 s and backgrounds for 5 s. Backgrounds were determined for each analysis point, and net Au and Fe count rates were converted to elemental concentrations using a ZAF correction procedure (Armstrong 1988, 1991). The Au and Fe metal standards were also analyzed as unknowns to ensure accurate and stable standardization. For the Au capsules used in petrologic experiments, analyses of Fe and Au were made every 20 μm across the thin, cylindrical portion of each capsule from 10 or 20 μm inboard of the partially molten sample to the outer edge.

EVIDENCE FOR Fe LOSS FROM MASS BALANCE

Phases produced in the experiments include melt plus plagioclase, amphibole, orthopyroxene, clinopyroxene, apatite, ilmenite, and zircon. Experimentally derived liquids are nearly homogeneous within each charge (even for Run 33, which lasted only 1 day), are rhyolitic to dacitic in composition, and have FeO(tot) contents ranging from 1.68 to 3.02 wt% (Table 3). The modal composition of each experiment was estimated by

weighted least-squares minimization, balancing the bulk composition of the starting material against the synthesized phase compositions (A.F. Glazner, written communication). Weighting factors were set equal to $1/s_i$, where s_i is the standard deviation for that oxide from representative microprobe analyses of the experimental run products. The failure of melt Fe concentrations to increase with greater degrees of melting was the first hint that Fe might have been lost during the experiments. Calculation of residuals for FeO that were far in excess of experimental errors reinforced this suspicion. Later mass-balance calculations that included a fictive FeO phase produced much smaller residuals, thereby indicating that Fe had indeed been lost from the samples. Estimates of Fe loss expressed as fictive FeO lost relative to the starting composition FeO(tot) are listed in Table 4 and compared with independent (but much less precise) estimates from microprobe analyses of Fe in the gold capsules.

Iron loss appears not to be a function of final run temperature (Fig. 1a). Instead, Fe loss from most of the experiments is inversely related to sample:capsule mass ratio (Fig. 1b), with the samples loaded in the medium and large capsules losing 16–20% of their total Fe, about half as much as that lost from

TABLE 3. Glass compositions (wt%) determined by electron microprobe analysis

Run	SiO$_2$	TiO$_2$	Al$_2$O$_3$	FeO(tot)	MnO	MgO	CaO	Na$_2$O	K$_2$O	P$_2$O$_5$	Cl	Orig. total	n
6	73.61(68)	0.20(13)	14.66(42)	1.68(17)	0.05(6)	0.42(19)	2.53(24)	3.42(16)	3.33(9)	0.06(5)	0.05(1)	90.88(67)	20
10	62.78(65)	1.24(27)	18.58(39)	3.02(25)	0.10(8)	2.27(16)	5.44(28)	3.79(23)	2.34(13)	0.41(6)	0.04(2)	92.27(127)	23
12	60.88(73)	1.54(15)	19.04(50)	2.95(24)	0.14(7)	3.10(19)	6.20(20)	3.77(20)	2.02(8)	0.33(5)	0.04(2)	94.39(108)	22
16	71.93(62)	0.34(14)	15.81(33)	1.70(25)	0.07(6)	0.56(26)	2.93(28)	3.64(15)	2.93(12)	0.05(4)	0.05(2)	92.04(80)	18
25	72.80(80)	0.25(14)	14.75(39)	2.15(15)	0.07(5)	0.51(11)	2.91(14)	3.10(28)	3.37(7)	0.05(4)	0.04(1)	91.48(111)	13
27	72.77(97)	0.24(18)	15.10(24)	2.05(19)	0.03(3)	0.48(8)	2.81(17)	3.14(13)	3.31(9)	0.04(3)	0.05(2)	91.49(98)	12
29	68.41(89)	0.43(21)	17.12(52)	2.96(29)	0.07(8)	0.62(8)	2.37(19)	4.43(22)	3.35(15)	0.17(7)	0.09(3)	90.10(102)	23
35	73.00(64)	0.26(13)	14.75(32)	1.99(21)	0.07(6)	0.37(6)	2.38(10)	2.74(16)	4.37(8)	0.05(3)	0.04(1)	91.29(70)	15

Notes: Bulk compositions have been normalized anhydrous to 100 wt%. Numbers in parentheses are 1-s deviations in the last decimal place from analyses of *n* melt pools.
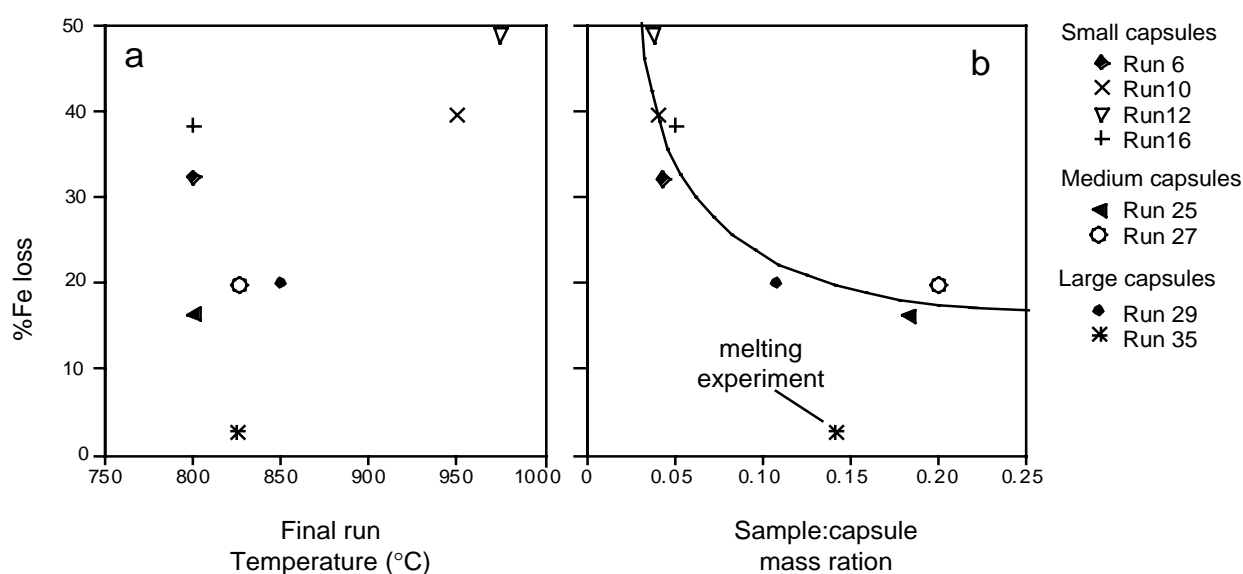

FIGURE 1. Iron loss, expressed as percent of total Fe, vs. (**a**) final run temperature and (**b**) sample:capsule mass ratio for experiments on YOS-55a hornblende quartz gabbro. Iron losses are calculated from mass balance of the run products.

TABLE 4. Estimates of Fe loss from mass-balance calculations and capsule analyses.

Run no.	% Fe loss from mass balance	% Fe loss from average Fe concentration in capsules
	1.4 mm capsule size	
Run 6	32.1	48
Run 10	39.5	23
Run 12	48.7	25
Run 16	38.2	42
	2.5 mm capsule size	
Run 25	16.0	11
Run 27	19.7	11
	4.0 mm capsule size	
Run 29	19.7	27
Run 33	*	31
Run 35	2.5	4

* Accurate mass balance was not possible due to heterogeneous phase compositions in this extremely short duration (1 day) experiment.

the small capsules (32–49%). An important exception from this general relationship is Run 35, the 825 °C melting experiment, the only experiment that was not subjected to high temperatures (≥970 °C). Iron losses in this experiment are minimal (<3% relative).

MICROPROBE ANALYSES OF FE IN USED CAPSULES

Analyses of virgin Au capsule materials (Table 5), not used for petrologic experiments, demonstrate that the capsules did not contain detectable quantities of Fe prior to experimentation. In contrast, all of the capsules used in the experiments contain measurable quantities of Fe (Fig. 2). Except for the medium and small capsules used in Runs 6 and 16, all of the capsules exhibit smooth gradients in Fe concentration with maxima near the inner wall closest to the sample. Results for the small capsule suggest that the slopes of these gradients decrease with run time. Two of the

experiments (Runs 25 and 27) produced thin (~20 μm), discontinuous Fe-rich rinds adjacent to the sample, but otherwise have relatively constant Fe concentrations immediately beyond these narrow zones. The identity of these rinds is unknown, but they are distinctly darker when viewed under reflected light compared to adjacent portions of the capsules. The rinds could result from cross-contamination between sample and capsule during polishing, they might be due to steep diffusion gradients, or they could be an as of yet unrecognized Fe-Au alloy. One of the medium capsules (Run 27) displays Fe concentrations that noticeably *increase* beyond ~400 μm from the sample. This pattern may be a remnant of a period of increased Fe diffusion during the 24 hours the experiment was held at 970 °C; however, it is difficult to reconcile this idea with the lack of similar gradients in other experiments. The large magnitude of Fe loss during the early high-temperature phase of the procedure is illustrated by the capsule analyses for Run 33 (one day at 970 °C), which approach 0.7 wt% Fe adjacent to the sample. In contrast, Fe concentrations within the capsule used in Run 35 (which was not taken to 970 °C) are significantly lower with most analyses, falling below 0.1 wt%.

Table 5. Analyses of standards and unused capsule material

Sample	Fe (wt%)	Au (wt%)	Total (wt%)
	Standards		
Au standard (n = 3)	0.00(0)	99.46(2)	99.46
Fe standard (n = 3)	100.23(7)	0.00(1)	100.23
	Unused capsules		
1.4 mm (n = 3)	0.00(0)	99.35(13)	99.35
2.5 mm (n = 3)	0.00(0)	99.31(13)	99.31
4.0 mm (n =3)	0.00(0)	99.37(12)	99.37

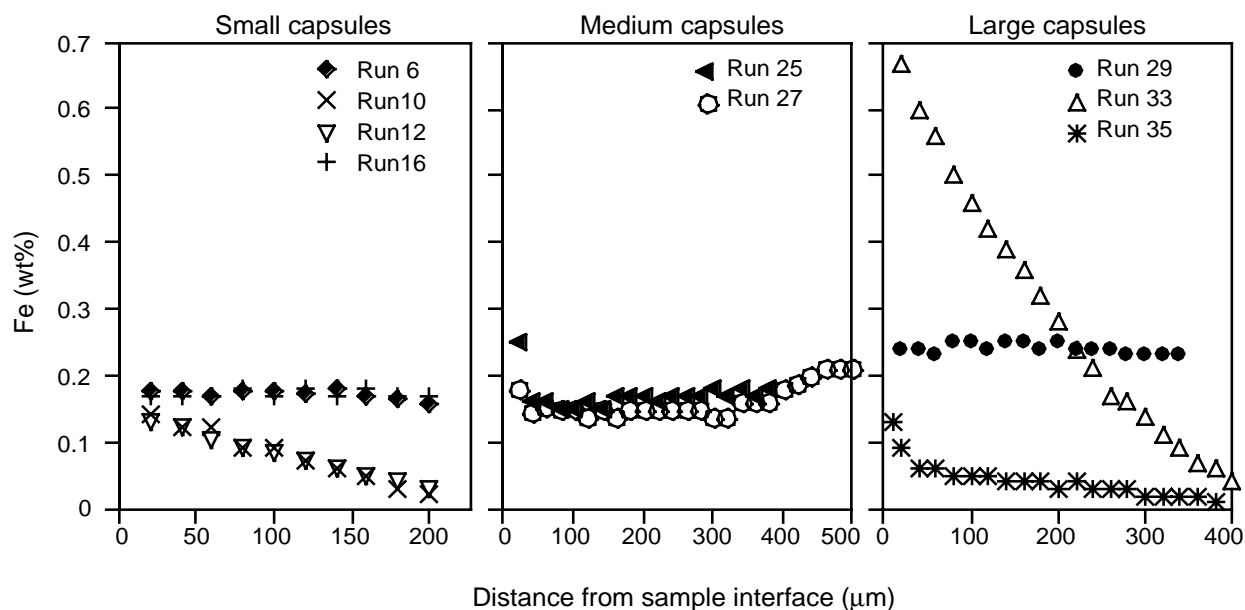*Note:* Uncertainties (1–s) in the last decimal place are given in parentheses.

FIGURE 2. Iron concentration gradients across Au capsules used in experiments. Symbols for experiments are the same as those in Figure 1. Uncertainties (1–s) for most analyses are ~2–3%, and are therefore smaller than the size of the symbols used in the figure.

Independent estimates of Fe losses were made using recorded sample and capsule weights and average Fe concentrations for each capsule. These estimates do not take into account asymmetries in Fe concentration gradients within the cylindrical walls of the capsules or different gradients at the capsule ends, and thus are very approximate. Nevertheless, results are generally within 50–200% of the Fe losses calculated from mass balance. These observations confirm that our samples lost Fe in the general amounts indicated by mass-balance calculations.

THERMODYNAMIC ANALYSIS

Because uptake of Fe into Au is not rate-limited by diffusion in the bulk sample, Fe loss from samples in Au capsules can be described by the reaction

$$FeO_{melt} \rightarrow Fe_{capsule} + 0.5O_2 \qquad (1)$$

The equilibrium constant for this reaction is

$$K = \frac{a_{Fe}^{capsule} \cdot (f_{O_2})^{0.5}}{a_{FeO}^{melt}} \qquad (2)$$

The large sub-solidus miscibility gap in the system Au-Fe shows that Fe and Au do not mix ideally. However, the low Fe concentrations produced in our Au capsules (<1 wt% Fe) are well within the Henry's law region on activity-concentration diagrams for Au-Fe alloys (Seigle 1956), where Fe activity is a linear function of Fe mole fraction. Use of Fe mole fraction, instead of Fe activity, is more convenient and modifies the value of K by a constant of proportionality, $1/\gamma^{Au}_{Fe}$.(the inverse of the activity coefficient for Fe in Au). Grove (1981) studied reaction 1 for the partitioning of Fe between silicate melt and Pt metal, and found that the oxide mole fraction of FeO in the melt, adjusted for melt $\frac{Fe^{3+}}{Fe^{2+}}$ at the experimental f_{O_2}, adequately described the activity of FeO in melt for equilibrium constant expression 2. Accordingly, we define an apparent equilibrium constant:

$$K' = \frac{X_{Fe}^{capsule} \cdot (f_{O_2})^{0.5}}{X_{FeO}^{melt}}. \qquad (3)$$

Microprobe analyses of quenched glasses and Au capsules were used to determine values of this apparent equilibrium constant. Published f_{O_2} estimates are near QFM-1 for samples run in piston-cylinder assemblies similar to those employed by us (Patiño Douce and Beard 1995), and we use QFM-1 to calculate melt $\frac{Fe^{3+}}{Fe^{2+}}$ after Kress and Carmichael (1991). Values of $X_{Fe}^{capsule}$ were taken from microprobe analyses immediately adjacent to the samples, or slightly inboard of the anomalously Fe-rich regions in the case of Runs 25 and 27. Finally, liquid compositions for each experiment were formulated as oxide mole fractions following normalization to 100 wt% anhydrous. Consistent K' values were derived for all the experiments except Run 33 (the unequilibrated, one-day experiment at 970 °C) and Run 35 (a melting experiment at 825 °C that contains significant amounts of unreacted sample and therefore also did not adequately approach equilibrium). The calculated K' values are strongly temperature-dependent (Fig. 3) and closely follow the equation:

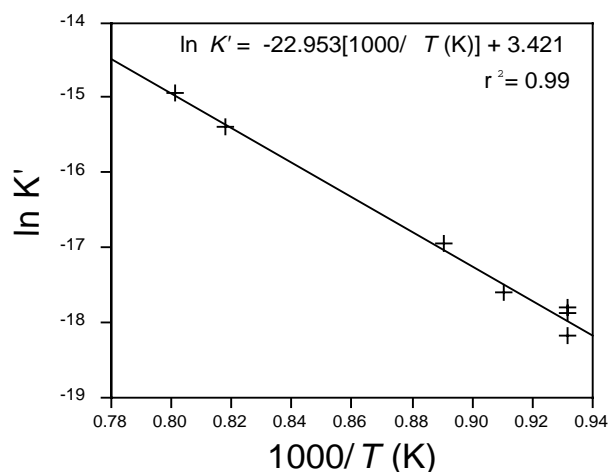$$\ln K' = -22.953[1000 / T(K)] + 3.421 \qquad (r^2 = 0.99) \qquad (4)$$

FIGURE 3. Ln K' vs. 1000/T (K) for experiments thought to have closely approached equilibrium (Runs 6, 10, 12, 16, 25, 27, and 29). Line shows result of linear regression.

This regression result is similar to that of Grove (1981) who obtained

$$\ln K = -20.727[1000 / T(K)] + 1.187 \qquad (r^2 = 0.89) \qquad (5)$$

for reaction 1 for the analogous case of Fe-Pt partitioning.

PRACTICAL APPLICATIONS

The limiting case of maximum Fe loss in a melting experiment will be that in which the sample is entirely molten and has reached complete equilibrium with its container. When the sample is entirely molten, all of the Fe is in the melt where it can diffuse rapidly and be absorbed by the container until equilibrium is reached. This limiting case is a useful guide for selecting an appropriate combination of experimental conditions to minimize or eliminate Fe loss. Using Equations 3 and 4, Fe losses were calculated for three representative basaltic, andesitic, and rhyolitic melts at a variety of temperatures, oxygen fugacities, and sample to capsule mass ratios, at 8 kbar pressure. Calculated Fe losses are not significantly different for the three compositions, and only the results for the basalt (USGS standard BHVO-1) are plotted in Figure 4 for varying temperatures at oxygen fugacities equivalent to QFM-1, NNO, and NNO + 2. Because of the strong curvature of the respective f_{O_2}-T buffer curves, petrologic samples that are subjected to oxygen fugacities constrained to these curves will lose more Fe at lower temperatures, despite the strong and opposite change in the value of the apparent equilibrium constant. In contrast, if oxygen fugacity is held at a constant value, Equation 4 predicts that experiments at high temperatures will lose more Fe than experiments at low temperatures.

The f_{O_2} values of common silicic magmas lie in the range of about 3 log units more reduced than the Ni-NiO buffer (NNO-3) to about 2.5 log units more oxidized than the Ni-NiO buffer (NNO + 2.5) (Carmichael 1991). For melting experiments toward the oxidized end of this array (~NNO + 2), potential Fe losses to Au are negligible (<2% relative) for sample to cap-
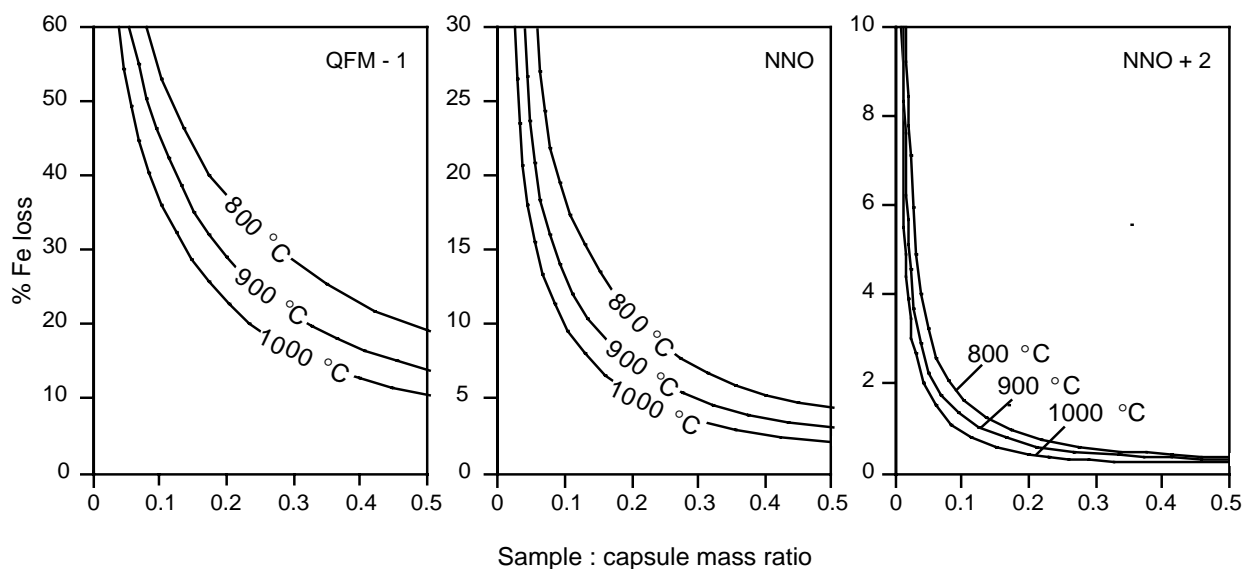
FIGURE 4. Percent Fe loss calculated for basaltic liquid (BHVO-1) as a function of sample:capsule mass ratio, temperature, and oxygen fugacity.

sule mass ratios greater than 0.08 at temperatures as low as 800 °C (Fig. 4). With effort, sufficient rock powder can be welded into a capsule as small as 1.4 mm diameter to attain a sample to capsule mass ratio above 0.08, so under oxidizing conditions, the loss of Fe to Au need not be a problem. At an f_{O_2} of NNO, keeping Fe loss to <10% relative is most safely ensured by using a sample to capsule mass ratio above ~0.2. Sample to capsule mass ratios of 0.2 or more can be obtained for thin-walled capsules as small as 2.5 mm diameter (Table 2), but would be difficult to achieve for smaller capsules. Under more-reducing conditions (f_{O_2} <QFM), keeping Fe loss below 10% relative would be difficult for any practical combination of sample and gold capsule masses (Fig. 4), in agreement with our mass-balance estimates of Fe loss (Table 5). This result is noteworthy because some combinations of sample and furnace assembly have been found to result in low f_{O_2} conditions (Patiño Douce and Beard 1995), and because graphitic or sulfidic starting materials, such as some sedimentary or metasedimentary rocks, will create low f_{O_2} conditions in melting experiments. Achieving low Fe loss in low f_{O_2} experiments may require pre-saturating the Au capsule stock with the appropriate amount of Fe, either by electroplating with Fe and annealing (Grove 1981), or by cleaning and re-using capsules. Equation 4 can be used to estimate the appropriate amount of Fe needed for the probable melt composition, oxygen fugacity, and temperature.

Because some piston-cylinder furnace configurations may impose low f_{O_2} conditions, and because some starting materials are inherently reducing, Fe loss to Au capsules may be more common than is widely appreciated. Results from previous and ongoing experimental studies in which samples have been taken to low f_{O_2} conditions may have to be re-examined for Fe loss. This problem is especially relevant to experiments that have produced Ti-poor magnetite as a run product, because the presence of a nearly pure Fe-oxide phase reduces the ability to de-

tect Fe loss by mass balance. Analyzing used capsules with the electron microprobe is a simple, precise, and expedient method to check for Fe loss. By examining a few used capsules an experimentalist can estimate the magnitude of potential Fe loss complications and decide if further investigations or modifications of the experimental setup are called for. If caught early, petrologic results can be improved significantly and a considerable waste of effort and materials can be avoided.

REFERENCES CITED

Armstrong, J.T. (1988) Quantitative analysis of silicate and oxide materials: Comparison of Monte Carlo ZAF, and *f*(rz) procedures. In D.E. Newburym Ed., Microbeam Analyses—1988, p. 239–246. SanFrancisco, California.

——(1991) Quantitative elemental analysis of individual microparticles with electron beam instruments. In K.F.J. Heinrich and D.E. Newbury, Eds., Electron Probe Quantation, p. 261–315. Plenum Press, New York.

Bohlen, S.R. (1984) Equilibria for precise pressure calibration and a frictionless furnace assembly for the piston-cylinder apparatus. Neues Jahrbuch Fur Geologie, Monatshefte, 9, 404–412.

Carmichael, I.S.E. (1991) The redox states of basic and silicic magmas: a reflection of their source regions? Contributions to Mineralogy and Petrology, 106, 129–141.

Gaetani, G.A. and Grove, T.L. (1998) The influence of water on melting of mantle peridotite. Contributions to Mineralogy and Petrology, 131, 323–346.

Grove, T.L. (1981) Use of FePt alloys to eliminate the iron-loss problem in 1-atmosphere gas mixing experiments: Theoretical and practical considerations. Contributions to Mineralogy and Petrology, 78, 298–304.

Kawamoto, T. and Hirose, K. (1994) Au-Pd sample containers for melting experiments on iron and water bearing systems. European Journal of Mineralogy, 6, 381–385.

Kress, V.C. and Carmichael, I.S.E. (1991) The compressibility of silicate liquids containing Fe_2O_3 and the effect of composition, temperature, oxygen fugacity and pressure on their redox states. Contributions to Mineralogy and Petrology, 108, 82–92.

Le Breton, N. and Thompson, A.B. (1988) Fluid-absent (dehydration) melting of biotite in pelitic rocks in the early stages of crustal anatexis. Contributions to Mineralogy and Petrology, 99, 226–237.

Merrill, R.B. and Wyllie, P.J. (1973) Absorption of iron by platinum capsules in high pressure rock melting experiments. American Mineralogist, 58, 16–20.

Nehru, C.E. and Wyllie, P.J. (1975) Compositions of glasses from St. Paul's peridotite partially melted at 20 kilobars. Journal of Geology, 83, 455–471.

Patiño Douce, A.E. and Beard, J.S. (1994) H_2O loss from hydrous melts during fluid-absent piston cylinder experiments. American Mineralogist, 79, 585–588.

———(1995) Dehydration-melting of biotite gneiss and quartz amphibolite from 3 to 15 kbar. Journal of Petrology, 36, 707–738.

Rapp, R.P. and Watson, E.B. (1995) Dehydration melting of metabasalt at 8–32 kbar: implications for continental growth and crust-mantle recycling. Journal of Petrology, 36, 891–931.

Seigle, L.L. (1956) Thermodynamic properties of solid Fe-Au alloys. Transactions of the American Institure of Mining and Metallurgical Engineers, 206, 91–97

Sisson, T.W. and Grove, T.L. (1993a) Experimental investigations of the role of H_2O in calc-alkaline differentiation and subduction zone magmatism. Contributions

to Mineralogy and Petrology, 113, 143–166.

———(1993b) Temperatures and H_2O contents of low-MgO high-alumina basalts. Contributions to Mineralogy and Petrology, 113, 167–184.

Skjerlie, K.P. and Johnston, A.D. (1996) Vapour-absent melting from 10 to 20 kbar of crustal rocks that contain multiple hydrous phases: implications for anatexis in the deep to very deep continental crust and active continental margins. Journal of Petrology, 37, 661–691.

Stern, C.R. (1973) Water-saturated and undersaturated melting relations of a granite to 35 kilobars. Earth and Planetary Science Letters, 18, 163–167.

Stern, C.R. and Wyllie, P.J. (1975) Effect of iron absorption by noble-metal capsules on hase boundaries in rock-melting experiments at 30 kilobars. American Mineralogist, 60, 681–689.

Truckenbrodt, J., Ziegenbein, D., and Johannes, W. (1997) Redox conditions in piston-cylinder apparatus: The different behavior of boron nitride and unfired pyrophyllite assemblies. American Mineralogist, 82, 337–344.

Vielzeuf, D. and Holloway, J.R. (1988) Experimental determination of the fluid-absent melting relations in the pelitic system. Consequences for crustal differentiation. Contributions to Mineralogy and Petrology, 98, 257–276.